Presented at the 23rd European Photovoltaic Solar Energy Conference and Exhibition, 1-5 September 2008, Valencia, Spain

ANALYZING THE EFFECTS OF LATERALLY VARYING EMITTER SHEET RESISTANCE IN COMBINATION WITH CONTACT RESISTANCE

D. Grote[1], M. Hermle[1], E. A. Wotke[1], U. Belledin[1], M. Hörteis[1], M. Spitz[1], M. Kasemann[2], S. Rein[1], D. Biro[1], W. Warta[1]
[1]Fraunhofer Institute for Solar Energy Systems (ISE), Heidenhofstr. 2, 79110 Freiburg, Germany
[2]University of Freiburg, Freiburg Material Research Center, Stefan-Meier-Str. 21, 79104 Freiburg, Germany
phone: +49 (0) 7 61 / 45 88-53 21, fax: +49 (0) 7 61 / 45 88-92 50, e-mail: daniela.grote@ise.fraunhofer.de

ABSTRACT: In this work the effect of a laterally varying emitter sheet resistance on IV characteristic parameters is analyzed for an industrial like solar cell structure by distributed circuit simulations. The influence of the emitter sheet resistance on contact resistance is considered by an experimentally determined dependence for screen printed contacts on shallow emitters with high surface doping concentration. Production solar cells with flaws in the distribution of the emitter sheet resistance as distinguished from e.g. cell structures with selective emitters are analyzed. In these cases the efficiency of a solar cell with laterally inhomogeneous emitter sheet resistance is decreased compared to the one of a solar cell with laterally homogeneous emitter sheet resistance with the mean value of the distribution. Nevertheless for solar cells with e.g. an emitter inhomogeneity of +/-20% on 20% of the cell area the decrease of efficiency is less than 0.15% relative in case of a moderate dependence between contact resistance and emitter sheet resistance. Hence a laterally inhomogeneous emitter influences the solar cell efficiency primarily by its effect on the contact formation during the firing step. Further effects are negligible.
Keywords: Modelling, Simulation, Emitter Sheet Resistance.

1 INTRODUCTION

Industrially fabricated silicon solar cells are large area devices, which currently have a cell area of typically 15.6 cm x 15.6 cm. Due to fluctuations in the diffusion furnace the emitter sheet resistance of such a solar cell may vary across the cell area. On the one hand a laterally inhomogeneous emitter may lead to contacting problems during the firing step. On the other hand the intrinsic properties of the laterally inhomogeneous emitter itself, i.e. the effective series resistance and the recombination properties, are expected to influence the efficiency of the finished solar cell.

In this contribution the last mentioned effects on solar cell results of industrially fabricated silicon solar cells are analyzed to estimate whether they affect the solar cell efficiency significantly in comparison to the influence of the contact formation during the firing process. Thereto distributed circuit simulations [1], [2], [3] are used.

To consider the influence of the emitter sheet resistance on contact resistance, an experimentally determined correlation for typical screen printed front contacts on highly doped shallow emitters is taken into account.

2 APPROACH

In this section the three dimensional distributed circuit model is introduced and the properties of the underlying local IV characteristics are presented.

2.1 The distributed circuit model

In Figure 1 the symmetry element used in our simulations is shown as well as a schematic of the equivalent circuit in direction perpendicular to the bus bar. For the distributed circuit simulations we used the circuit simulation program LTspice / Switcher CADIII [4].

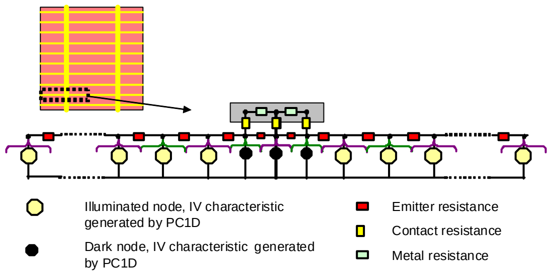

Figure 1: Symmetry element and schematic of the equivalent circuit in direction perpendicular to the bus bar used in the distributed circuit simulations.

The used distributed circuit model neglects lateral diffusion of minority carriers, which is intrinsic for this kind of model, and lateral diffusion of majority carriers in the base. Therefore the validity of this assumption in the case of laterally inhomogeneous emitter sheet resistances was analyzed using Sentaurus Device [5] simulations (see [6], chapter 3.4.3, or [7], chapter 3.4). The results show, that the effects of inhomogeneous emitter sheet resistances on solar cell results may be simulated in good approximation by distributed circuit simulations.

Furthermore distributed series resistance effects, e.g. of the emitter, have to be taken into account when performing distributed circuit simulations [8]. Therefore the resolution of the distributed circuit models used in this paper was set high enough to obtain comparable results.

2.2 The baseline models

The local IV characteristics used in the distributed circuit model were generated using PC1D [9]. An industrial like silicon solar cell was chosen with an n-doped emitter, a thickness of 180 µm, a textured surface and a SiN antireflection coating. The p-doped base resistivity was set to 3 Ohm cm, the bulk lifetime to 90 µs, which represents a Cz solar cell with high bulk lifetime [10]. At the rear a screen printed aluminum back surface field according to [11] was chosen with a constant doping concentration of 2×10^{19} cm^{-3} and a depth of 12 µm. The parameter J_{02} was set to 10^{-8} A/cm^2.

As emitter profiles the profiles of complementary error functions were chosen, in order to realize a wide variety of emitter types. Measured profiles for such a wide range are not available. These profiles differ from actual profiles obtained by diffusing phosphor into silicon (e.g. [12]), but serve as a convenient basis to estimate the effects.

The influence of the emitter sheet resistance on the IV-characteristics was analyzed by varying

- the PC1D depth factor and holding the front surface concentration constant. The front surface doping concentration was set to $N_{front} = 1.9 \times 10^{20}$ cm^{-3}. This results in a variation of the junction depth between 0.13 µm and 0.65 µm for emitter sheet resistances between 125 Ohm/sq and 25 Ohm/sq.
- the front surface doping concentration. The PC1D depth factor was set to 0.15015 µm, which results in front surface doping concentrations between 4.2×10^{20} cm^{-3} and 6.2×10^{19} cm^{-3} for emitter sheet resistances between 25 Ohm/sq and 125 Ohm/sq.

In both cases the front surface recombination velocity was determined according to [13] under consideration of a factor three due to the textured front surface [14]. The peak position was located at the front surface. Figure 2 shows examples of the used profiles.

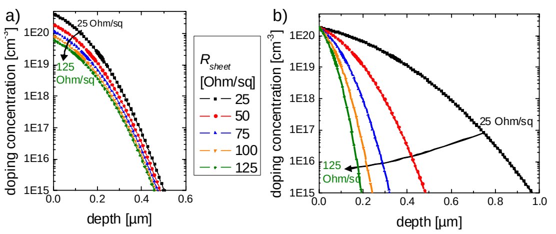

Figure 2: Examples of the used emitter profiles (complementary error function);
a) Varying front surface doping concentration;
b) Varying emitter depth.

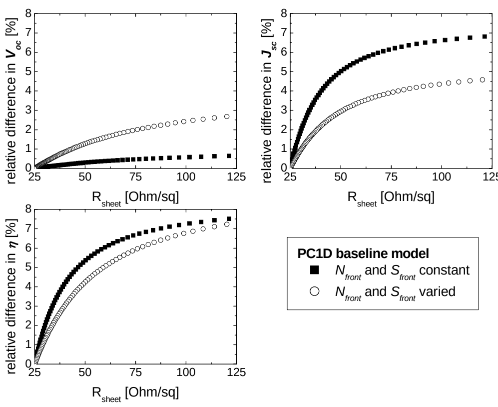

Figure 3: Relative difference of the IV characteristic parameters V_{oc}, J_{sc} and efficiency compared to the PC1D-baseline cell with an emitter sheet resistance of 25 Ohm/sq.

In Figure 3 the relative difference of the IV characteristic parameters V_{oc}, J_{sc} and efficiency compared to the PC1D-baseline cell with an emitter sheet resistance of 25 Ohm/sq is shown.

J_{sc} is influenced more than V_{oc} due to the decreasing Auger-recombination with increasing emitter sheet resistance close to the pn-junction. The combined variation of S_{front} and N_{front} results in a higher increase in V_{oc} than the variation of the emitter depth. The gradient in all parameters decreases with increasing emitter sheet resistance.

2.3 Dependence between emitter sheet resistance and contact resistance

The contact resistance depends on the surface concentration of the doping [15]. The contact resistances of conventional screen printed contacts are usually much higher than the contact resistances given in [15] ([16], Table 2.1). Therefore the dependence of the contact resistance on the emitter sheet resistance was determined for Czochralski (Cz) solar cells with random pyramids and acidly textured multicrystalline (mc) solar cells with industrial like shallow emitters with high surface doping concentration (between 10^{20} cm^{-3} and 10^{21} cm^{-3}) and screen printed front contacts. All contacts were fired under equal conditions. The results are shown in Figure 4.

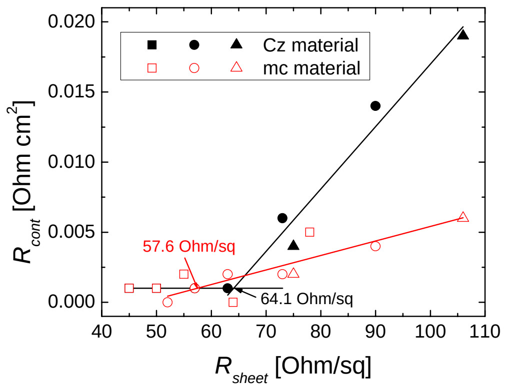

Figure 4: Dependence of the contact resistance on the emitter sheet resistance, determined for Cz and mc solar cells with industrial like emitters and screen printed front contacts. The same symbols are used for emitters obtained by the same deposition and drive in times, but using different temperatures. All contacts were fired at the same temperature.

The contact resistance at the mc-material shows only a minor dependence on the emitter sheet resistance.

To estimate a range of the influence of the emitter sheet resistance in correlation with contact resistance on solar cell parameters the distributed circuit simulations were carried out using the dependence determined for the Cz wafers. This is

$R_{sheet} > 64$ Ohm/sq:

$$R_{cont} = -0.0275\,\text{Ohm cm}^2 + 4.45 \times 10^{-4}\,\text{cm}^2 \cdot R_{sheet} \quad (1)$$

$R_{sheet} \leq 64$ Ohm/sq:

$$R_{cont} = 0.001\,\text{Ohm cm}^2 .$$

It has to be kept in mind, that the results in this paper are based on dependence (1), which is individual for the process analyzed. Especially for emitters with lower front surface concentration the dependence between contact resistance and emitter sheet resistance will show a steeper slope.

Furthermore no shunting problems are taken into account, which might occur in the case of shallow emitters and high contact firing temperatures.

3 DISTRIBUTED CIRCUIT SIMULATIONS

The distributed circuit simulations of laterally inhomogeneous emitter sheet resistances were carried out for three levels of emitter sheet resistances: 50, 75 and 100 Ohm/sq.

The different emitter sheet resistances were achieved by varying

- the PC1D depth factor and holding the front surface concentration constant
- the front surface concentration (and front surface recombination velocity).

Details about the profiles are given in 2.2.

3.1 Laterally homogeneous emitter sheet resistances

Optimization of the distance between two adjacent fingers

Real solar cells are usually fabricated with the optimum distance between two adjacent fingers aiming at maximum solar cell efficiency. Therefore for the three analyzed emitter sheet resistances the distance between two adjacent fingers was varied and the distance, which results in the highest efficiency, was used in the further simulations. The results are given in Table I. Further solar cell parameters, which were used in all distributed circuit simulations, are given in Table II. They were chosen to represent industrial silicon solar cells with conventional screen printed front contacts.

Table I: Optimum distance between two adjacent fingers, determined for the baseline model with emitter sheet resistances with an electrical active front surface doping concentration of 1.9×10^{20} cm^{-3}. Further parameters are given in Table II.

R_{sheet} [Ohm/sq]	50	75	100
Opt. distance between two adjacent fingers [mm]	2.2	1.9	1.7

Table II: Parameters used in all distributed circuit simulations.

Length of the fingers between bus bar and edge of the symmetry element	[cm]	3.8
Width of the bus bar	[mm]	2
Width of the finger	[µm]	100
Height of the metallization (bus bar and finger)	[µm]	15
Position of the measurement node	In the middle of the symmetry element	
Specific resistivity of the metallization	[Ohm cm]	3.2×10^{-6}

Influence of the surface recombination velocity beneath the front contacts on IV characteristic parameters

In a first step the influence of the front surface recombination velocity beneath the front contacts on the IV characteristic parameters was analyzed.

For this purpose the distributed circuit simulations were performed once using a surface recombination velocity of 57 000 cm/s for the whole solar cell, i.e. also in the metalized regions (black squares in Figure 5), and once substituting the baseline models in the metalized regions by ones with surface recombination velocities of 10^7 cm/s (red circles in Figure 5). This corresponds to the thermal velocity in n-type <111> silicon (more precisely: 5.2×10^6 cm/s, see [17], chapter 5.4.3). The emitter sheet resistance was varied by varying the emitter depth factor.

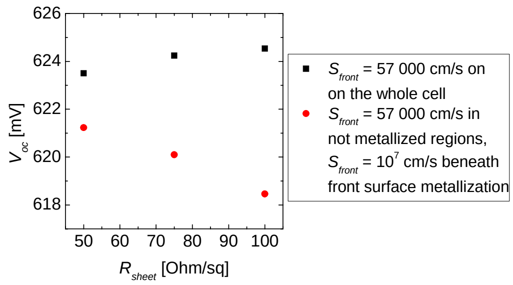

Figure 5: Comparison between distributed circuit simulations with and without adjusted front surface recombination velocity beneath the front surface metallization.

Without consideration of the increased surface recombination velocity beneath the metallization V_{oc} increases with increasing emitter sheet resistance, while V_{oc} decreases, when it is taken into account.

Therefore the simulations in the following sections take the effect of increased surface recombination velocity beneath the metallization into account.

Comparison between the two types of emitter sheet resistance variation

In a second step the IV characteristic parameters obtained with circuit simulation by increasing the emitter sheet resistance once by decreasing the surface concentration (grey bars in Figure 6) and once by decreasing the emitter depth (red striped bars in Figure 6) are compared for laterally homogeneous emitter sheet resistances.

For both kinds of variation J_{mpp} at first increases with increasing emitter sheet resistance, which is due to the increasing current density in the baseline models, and decreases with further increasing emitter sheet resistance, which is due to the increasing fraction of metalized front.

V_{mpp} decreases in both kinds of variation with increasing emitter sheet resistance due to an increase in effective series resistance. In the case of decreasing front surface doping concentration the decrease is smaller due to the correlated decrease in front surface recombination velocity.

As result the efficiency in the last mentioned case at first increases slightly, before it decreases with further increasing emitter sheet resistance. In the other case the increase in J_{mpp} is overcompensated by the decrease in

V_{mpp}, which results in a decreasing cell efficiency with increasing emitter sheet resistance.

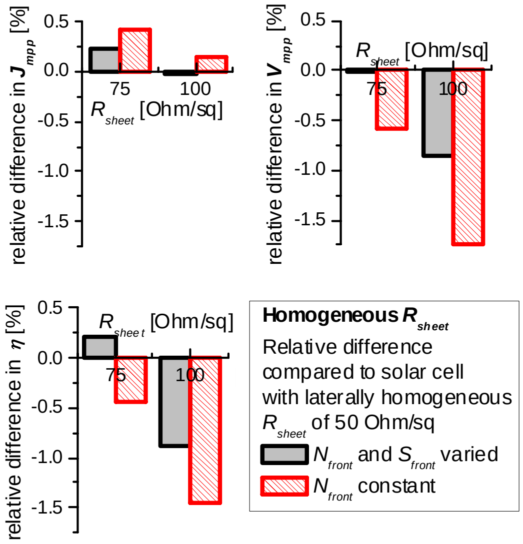

Figure 6: Results of the distributed circuit simulations with laterally homogeneous R_{sheet}. Relative difference in IV characteristic parameters to a laterally homogeneous emitter sheet resistance of 50 Ohm/sq. The emitter sheet resistance was varied once by varying the front surface concentration and once by varying the depth factor in the PC1D baseline model.

3.2 Laterally inhomogeneous emitter sheet resistances

Figure 7 shows the two structures which were used to analyze the effect of a laterally inhomogeneous emitter sheet resistance. For simplicity only three different emitter sheet resistances were used. In structure 1, the contact resistance may be influenced by the varying emitter sheet resistance. This structure may occur in a diffusion furnace with laterally inhomogeneous temperature distribution or gas flow. Structure 2, which is quite artificial for real solar cells, was used to simulate the effect of a laterally inhomogeneous emitter sheet resistance, whose inhomogeneity is not connected to the front contacts.

The area share in total area with $R_{sheet,1}$ or $R_{sheet,2}$ is 19.5% in structure 1, in structure 2 it is 21.0%. The area share in metalized area is 12.5% for the metalized regions with $R_{sheet,1}$ or $R_{sheet,2}$ in structure 1.

The emitter sheet resistance in all simulations was distributed symmetrically, which means

$$\begin{aligned} R_{sheet,1} &= R_{sheet,2} - \Delta R_{sheet} \\ R_{sheet,3} &= R_{sheet,2} + \Delta R_{sheet} \end{aligned} \tag{2}$$

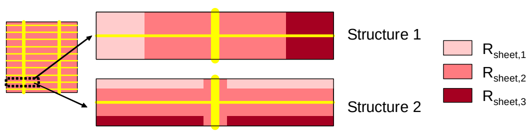

Figure 7: Two structures used to analyze the effect of laterally inhomogeneous emitter sheet resistance.

Two strengths in inhomogeneity were analyzed:

ΔR_{sheet} = 20% $R_{sheet,2}$

ΔR_{sheet} = 25 Ohm/sq.

Already the first one represents a quite strong inhomogeneity compared to the ones which occur on real solar cells. But as will be seen in the next paragraph, the influence on solar efficiency is quite low. Therefore the second strength was analyzed to consider more grave effects.

Figure 8 shows the effect of these inhomogeneities on cell efficiency compared to a solar cell with laterally homogeneous emitter sheet resistance.

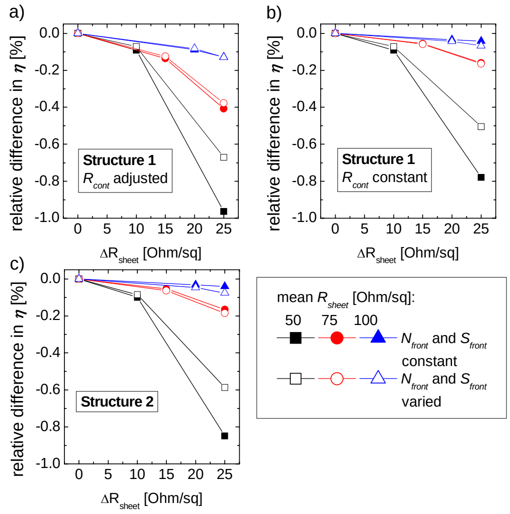

Figure 8: Relative difference in efficiency compared to a solar cell with laterally homogeneous emitter sheet resistance. For structure 1, the simulations were carried out with (a) and without (b) adjusting the contact resistivity.

All simulation results show a decrease in efficiency compared to the homogeneous case. As emitter sheet resistance distributions, which are symmetrical to their mean value, were assumed, this is due to the fact, that the efficiency loss towards lower emitter sheet resistances is higher than the efficiency gain towards higher emitter sheet resistances in the underlying baseline models (Figure 3). Furthermore the dependence between contact resistance and emitter sheet resistance considered in this paper (see equation (1)) is moderate.

The efficiency decrease solely due to emitter sheet resistance (Figure 8 b) and Figure 8 c)) is stronger in the case of lower emitter sheet resistances than of higher ones. This is caused by the steeper slopes of the underlying baseline model in the regions of lower emitter sheet resistances.

The efficiency loss for the simulations with an inhomogeneity of ΔR_{sheet} = 20% is less than 0.15% relative in all cases, which is less than the achievable measurement accuracy.

The effect of structure 1 without adjusting the contact resistance (Figure 8 b) and structure 2 (Figure 8 c) on solar cell efficiency is very similar. The distributed circuit simulations confirm that in cases, when only the emitter sheet resistance varies, the emitter sheet resistance distribution and an appropriate averaging method is sufficient to calculate the effect on the solar cell IV characteristics ([6], chapter 3.4.3). The different non generation losses in structure 1 and 2, which are considered in the distributed circuit simulations, appear to be negligible for the regarded solar cells structures.

If the dependence between emitter sheet resistance and contact resistance according to equation (1) is considered, the decrease in efficiency towards higher emitter sheet resistances and higher variations in emitter sheet resistance is increased (Figure 8 a) compared to Figure 8 b)). In the case of varying front surface concentration (open symbols) the effect is probably underestimated in comparison to real solar cells as here the increase in contact resistance with increasing emitter sheet resistance might be steeper.

4 CONCLUSIONS

In the case of a moderate relation between contact resistance and emitter sheet resistance, a distribution of emitter sheet resistances symmetrical to its mean value results in a decrease in cell efficiency compared to a solar cell with a laterally homogeneous emitter sheet resistance with the mean value.

In the analyzed cases the efficiency loss due to a laterally inhomogeneous emitter sheet resistance with a variation of +/-20% on a cell area of 20% is less than 0.15%, which is less than the measurement accuracy. The effect may be increased when the emitter profiles differ from the analyzed ones or the contact resistance shows a stronger dependence on emitter sheet resistance.

Hence a laterally inhomogeneous emitter influences the solar cell efficiency primarily by its effect on the contact formation during the firing step. The technological window for optimized firing conditions without shunting to occur is expected to become narrower, but the effects investigated here are negligible.

ACKNOWLEDGEMENTS

This work was funded by the German Ministry for the Environment, Nature Conservation and Nuclear Safety (contract number 0327616 (PVQC)).

REFERENCES

[1] J. Dicker, J. Isenberg and W. Warta, Proceedings of the 17th European Photovoltaic Solar Energy Conference, Munich, Germany (2001) 1567.
[2] P.O. Grabitz, U. Rau and J.H. Werner, physica status solidi (a) 202 (2005) 2920.
[3] B. Galiana, C. Algora, I. Rey-Stolle and I.G. Vara, IEEE Trans. Electron Devices 52 (2005) 2552.
[4] M. Engelhardt. Linear Technology Corporation 2007.
[5] Synopsys TCAD (2007) http://www.synopsys.com.
[6] J. Isenberg, Neue Infrarotmesstechniken der Photovoltaik, PhD-Thesis, Universität Konstanz, Konstanz, 2003.
[7] D. Grote, Analyse und Modellierung lateral variierender Eigenschaften industriell hergestellter Solarzellen, Diploma Thesis, Universität Freiburg, Freiburg, 2004.
[8] D. Grote, M. Kasemann, M. Hermle and W. Warta, Proceedings of the 22nd European Photovoltaic Solar Energy Conference, Milan, Italy (2007) 305.
[9] D.A. Clugston and P.A. Basore, Proceedings of the 26th IEEE Photovoltaic Specialists Conference, Anaheim, California, USA (1997) 207.
[10] S. Rein, W. Warta and S.W. Glunz, Proceedings of the 28th IEEE Photovoltaics Specialists Conference, Anchorage, Alaska, USA (2000) 57.
[11] F. Huster and G. Schubert, Proceedings of the 20th European Photovoltaic Solar Energy Conference, Barcelona, Spain (2005) in print.
[12] A. Bentzen, Phosphorus diffusion and gettering in silicon solar cells, PhD-Thesis, University of Oslo, Oslo, 2006.
[13] A. Cuevas, G. Giroult-Matlakowski, P.A. Basore, C. DuBois and R.R. King, Proceedings of the 1st World Conference on Photovoltaic Energy Conversion- WCPEC, Waikoloa, Hawaii, USA (1994) 1446.
[14] J. Dicker, Charakterisierung von hocheffizienten Rückseitenkontaktzellen, Diplomarbeit, Albert-Ludwigs-Universität, Freiburg, Freiburg, 1998.
[15] D.K. Schroder and D.L. Meier, IEEE Transactions on Electron Devices ED-31 (1984) 637.
[16] A. Mette, D. Pysch, G. Emanuel, D. Erath, R. Preu and S.W. Glunz, Progress in Photovoltaics: Research and Applications 15 (2007) 493.
[17] S.M. Sze, Physics of Semiconductor Devices, 2nd ed., John Wiley & Sons, New York, 1981.